

Autohydration of Nanosized Cubic Zirconium Tungstate

Nathan A. Banek, Hassan I. Baiz, Akena Latigo, and Cora Lind*

Department of Chemistry, The University of Toledo, Toledo, Ohio 43606

Received February 19, 2010; E-mail: cora.lind@utoledo.edu

Negative thermal expansion (NTE) materials have attracted widespread interest due to their potential applications as fillers in controlled thermal expansion composites and coatings.^{1–11} High quality composites require small, homogeneous particles that are stable in their environment. To date, cubic zirconium tungstate (ZrW_2O_8) has been considered one of the most promising NTE materials. Here we report that nanosized ZrW_2O_8 absorbs atmospheric moisture under ambient conditions, resulting in formation of a hydrated material and loss of NTE character.

Micron sized cubic ZrW_2O_8 has been incorporated into ceramic composites for optical fiber coatings and grating supports to minimize spectral shifts caused by thermal expansion.^{12,13} This NTE material possesses a number of desirable properties, including a wide temperature range of isotropic expansion with α values of $-8.8 \times 10^{-6} \text{ K}^{-1}$ from 0.3 to 430 K and $-4.9 \times 10^{-6} \text{ K}^{-1}$ from 430 to 1050 K.^{1,2} ZrW_2O_8 is part of the AM_2O_8 ($A = \text{Zr, Hf; M} = \text{Mo, W}$) family of materials,^{2,14,15} in which the oxygens in the linear $\text{M}-\text{O}-\text{M}$ bonds undergo transverse vibrations, causing a decrease in unit cell volume.^{16,17}

The preparation of high quality composites requires a homogeneous distribution of filler particles, making small particles with uniform particle morphology favorable for such applications. The first reported synthesis of ZrW_2O_8 used sintering of WO_3 and ZrO_2 at 1473 K for 15 min, followed by rapid quenching in water.¹⁸ The quenching step is necessary to avoid decomposition into binary oxides, as ZrW_2O_8 is only thermodynamically stable between 1380 and 1530 K and metastable below 1050 K.¹ It was later shown that ZrW_2O_8 is accessible at low temperatures by dehydration of a precursor, $\text{ZrW}_2\text{O}_7(\text{OH})_2 \cdot 2\text{H}_2\text{O}$, followed by topotatic recrystallization. This hydroxide hydrate was originally obtained by reflux or hydrothermal treatment in HCl .^{19,20} The synthesis can also be carried out in other acids, however, the crystallization kinetics depend strongly on hydronium and chloride ion concentration.²¹ Changes in solution composition can be used to influence the final particle size through controlled variation of nucleation and growth rates. Small particles could be obtained by substituting HClO_4 for HCl and adding NaCl as a chloride source,²² but the particles were highly agglomerated. It was necessary to overcome this agglomeration problem, as it interferes with the preparation of high quality homogeneous composites. It was found that reactions in alcohol/ HCl mixtures significantly reduced agglomeration while maintaining small particle sizes. Optimized particles were obtained from 2.7 M 1-butanol/7 M HCl mixtures, resulting in rods that were 15–50 nm wide by 200–500 nm long, and formed agglomerates of 50–100 nm by 300–600 nm.

In an attempt to further reduce agglomeration additional alcohols were investigated. Small particles with reasonable agglomeration were obtained for alcohol chain lengths of 3–5 carbons. To our surprise, nanoparticles of cubic ZrW_2O_8 prepared in these acid/alcohol mixtures were significantly less stable than those prepared in the absence of alcohols. In this paper, we report that nanosized ZrW_2O_8 particles show autohydration under ambient conditions.

This observation has significant implications for the potential use of ZrW_2O_8 as an NTE filler in composites, as insertion of water into the framework results in weak positive thermal expansion. For micrometer sized particles, this hydrate formation under ambient conditions was previously only observed for mixed zirconium tungstate molybdates with 30 to 90% tungsten content,^{23,24} while hydrothermal treatment in water at 180 °C was necessary to force water into pure ZrW_2O_8 .

A hydrothermal method in acid/alcohol mixtures was used to obtain $\text{ZrW}_2\text{O}_7(\text{OH})_2 \cdot 2\text{H}_2\text{O}$.²² The starting materials, 0.450 g of $\text{ZrOCl}_2 \cdot x\text{H}_2\text{O}$ and 0.660 g of $\text{NaWO}_4 \cdot 2\text{H}_2\text{O}$, were each dissolved in 1.25 mL of distilled H_2O . Upon addition to a 23 mL Parr bomb filled with 2.5 mL of 2-pentanol, a white precipitate formed. After stirring for 5 min, 5 mL of concentrated HCl were added, and the Parr bomb was sealed and placed into an oven at 130 °C for 24 h. The $\text{ZrW}_2\text{O}_7(\text{OH})_2 \cdot 2\text{H}_2\text{O}$ precursor was centrifuged, washed with distilled H_2O , and dried at 60 °C. The white powder was heat treated at 600 °C for 30 min to form crystalline cubic ZrW_2O_8 .

Powder X-ray diffraction experiments were performed on a PANalytical X'Pert Pro diffractometer equipped with an X'Celerator detector. Scans were collected shortly after heat treatment, as well as several weeks to several months after initial formation of ZrW_2O_8 . Thermogravimetric/differential thermal analysis (TG-DTA) was carried out on a TA Instruments SDT 2960 Simultaneous TGA-DTA. Particles were imaged on a Hitachi HD-2300 scanning transmission electron microscope (STEM) with an accelerating voltage of 200 kV.

Powder X-ray diffraction on the as recovered material showed a single phase pattern corresponding to $\text{ZrW}_2\text{O}_7(\text{OH})_2 \cdot 2\text{H}_2\text{O}$. The crystallite size was estimated using the Scherrer equation after correcting for the instrument contribution as determined with a silicon standard. An average size of 20–25 nm was obtained for all samples. STEM analysis showed rod shaped particles with size ranges of 15–80 nm wide by 150–600 nm long. The particles formed agglomerates of 150–300 nm by 500–1500 nm. Heat treatment to 600 °C resulted in a weight loss corresponding to 3 water molecules. An X-ray pattern collected several days after heat treatment showed broad peaks and some signs of peak splitting (Figure 1b). It was apparent that several reflections remained single peaks, while other features were best fit as an overlap of two peaks. The pattern could be described by two cubic phases with lattice constants of approximately 9.12 and 8.95 Å, with several reflections absent in the smaller cell. The lattice constant of cubic ZrW_2O_8 has been reported as ~ 9.14 Å, which is similar to the larger cell. The lattice constant of the smaller cell, and the absence of certain reflections, resembled Duan's report of a partially hydrated $\text{ZrW}_2\text{O}_8 \cdot x\text{H}_2\text{O}$ phase. The sample was monitored over a period of several months. During this time, the peaks continued to shift to higher angles and ultimately formed a single cubic phase with a lattice constant of 8.91 Å (Figure 1c). The (111), (221), and (310) peaks were absent in this phase. To verify that the changes in the pattern were due to hydration, the sample was reheated to 200 °C for 30 min, and an X-ray pattern was collected immediately after cooling. A single cubic phase

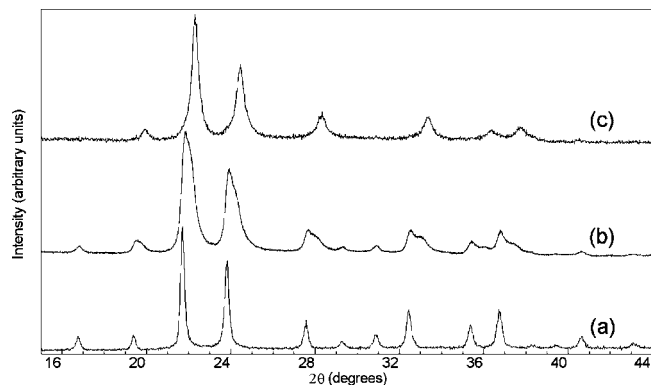


Figure 1. Powder X-ray patterns of ZrW_2O_8 (a) as prepared (no hydration), (b) after a few days (partially hydrated), (c) after 1 year (close to fully hydrated).

with a lattice constant of 9.14 \AA was observed (Figure 1a). The width of the peaks corresponded to an average crystallite size of $25\text{--}30 \text{ nm}$.

Hydrated cubic $\text{ZrW}_2\text{O}_8 \cdot x\text{H}_2\text{O}$ was first prepared by Duan et al. by hydrothermal treatment.²³ Full hydration of zirconium tungstate results in a linear decrease in lattice constant from 9.14 \AA in ZrW_2O_8 to 8.84 \AA in $\text{ZrW}_2\text{O}_8 \cdot 1\text{H}_2\text{O}$. Hydration results in an increase in the tungsten coordination number from 4 to 5 and a change in space group from $P2_13$ to $Pa\bar{3}$. This higher coordination number leads to rotations of the WO_5 and ZrO_6 units, causing further contraction of the unit cell. The extent of autohydration of nano- ZrW_2O_8 can be estimated using the lattice constant relationship found by Duan et al. The lattice constant of a sample exposed to the atmosphere for 1 year, 8.91 \AA , should correspond to a hydration level of $\text{ZrW}_2\text{O}_8 \cdot 0.75\text{H}_2\text{O}$. TG-DTA analysis showed a steep mass loss between 100 and $140 \text{ }^\circ\text{C}$ and a non-negligible mass loss between room temperature and $100 \text{ }^\circ\text{C}$. The total mass loss of 2.20% corresponds to a composition of $\text{ZrW}_2\text{O}_8 \cdot 0.73\text{H}_2\text{O}$, which is in good agreement with the water content suggested by the lattice constant.

The particles of corresponding hydroxide hydrate and cubic phases were imaged in an electron microscope. It was previously reported that the particle size and shape of the precursor are preserved during the conversion to cubic ZrW_2O_8 . Surprisingly, significant changes in particle morphology were observed for some of the heat treated samples in this study (Figure 2). The individual rods of the hydroxide hydrate appear to fuse together, forming larger entities without distinct particle boundaries in the cubic phase. This suggests that the particles of the precursor contain a significant number of defects, which present high energy sites that facilitate the fusion process. These defects may also play an important role in the observed autohydration behavior. Micron sized ZrW_2O_8 particles with low defect concentrations do not react with atmospheric moisture, while autohydration has been reported for micrometer sized mixed cation $\text{ZrW}_{2-x}\text{Mo}_x\text{O}_8$ compositions, which are likely to contain more defects than pure ZrW_2O_8 or ZrMo_2O_8 . The kinetics of autohydration are related to the surface area of the particles. Micron sized ZrW_2O_8 as well as nanoparticles prepared in the absence and presence of alcohols showed BET surface areas of 4.75 , 6.46 , and $18.99 \text{ m}^2/\text{g}$, respectively. The fact that no hydration was observed in the micrometer sized particles, while slow autohydration occurred in the nanoparticles prepared without alcohols, suggests that defects determine whether autohydration occurs while the surface areas dictate the kinetics. Samples prepared in the presence of alcohols showed considerable hydration after a period of a few weeks, while samples with similar particle sizes prepared in the absence of alcohols only reached a comparable degree of hydration after several months.

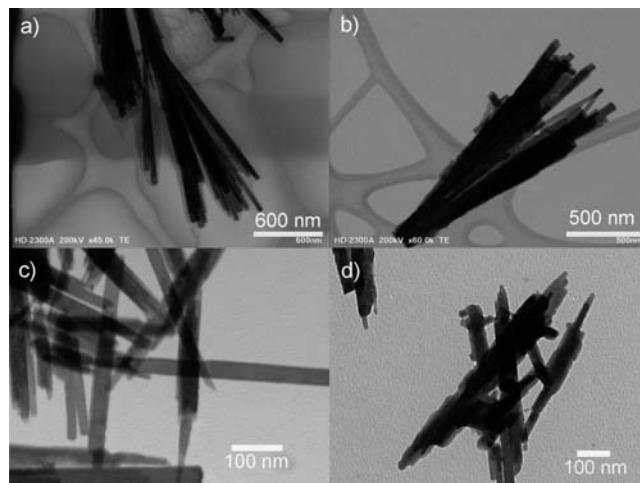


Figure 2. Scanning transmission electron micrographs of (a) $\text{ZrW}_2\text{O}_7(\text{OH})_2 \cdot 2\text{H}_2\text{O}$ and (b) ZrW_2O_8 prepared by perchlorate route; (c) $\text{ZrW}_2\text{O}_7(\text{OH})_2 \cdot 2\text{H}_2\text{O}$ and (d) ZrW_2O_8 prepared in 1-butanol/HCl.

The autohydration of nanosized cubic ZrW_2O_8 imposes serious limitations on the potential use of this compound as a filler in controlled thermal expansion composites. Further studies are underway to gain a detailed understanding of the effect of defects on this behavior and to optimize processing conditions to minimize or prevent autohydration.

Acknowledgment. This research was supported through NSF Grant DMR-0545517. A.L. acknowledges support through ACS Project SEED. We thank Q. Yao for BET measurements.

References

- Mary, T. A.; Evans, J. S. O.; Vogt, T.; Sleight, A. W. *Science* **1996**, *272*, 90.
- Evans, J. S. O.; Mary, T. A.; Vogt, T.; Subramanian, M. A.; Sleight, A. W. *Chem. Mater.* **1996**, *8*, 2809.
- Atfield, M. P.; Sleight, A. W. *Chem. Mater.* **1998**, *10*, 2013.
- Korthuis, V.; Khosrovani, N.; Sleight, A. W.; Roberts, N.; Dupree, R.; Warren, W. W. *Chem. Mater.* **1995**, *7*, 412.
- Ernst, G.; Broholm, C.; Kowach, G. R.; Ramirez, A. P. *Nature* **1998**, *396*, 147.
- Mittal, R.; Chaplot, S. L.; Schober, H.; Mary, T. A. *Phys. Rev. Lett.* **2001**, *86*, 4692.
- Ramirez, A. P.; Kowach, G. R. *Phys. Rev. Lett.* **1998**, *80*, 4903.
- Evans, J. S. O.; Hu, Z.; Jorgensen, J. D.; Argyriou, D. N.; Short, S.; Sleight, A. W. *Science* **1997**, *275*, 61.
- Perottoni, C. A.; da Jornada, J. A. H. *Science* **1998**, *280*, 886.
- Sleight, A. W. *Annu. Rev. Mater. Sci.* **1998**, *28*, 29.
- Evans, J. S. O.; Mary, T. A.; Sleight, A. W. *J. Solid State Chem.* **1997**, *133*, 580.
- Hui-Ling, W.; John, L.; Yu-Lung, L. U.S. Patent 6,936,235, August 30, 2005.
- Fleming, D. A.; Johnson, D. W.; Lemaire, P. J. U.S. Patent 5,694,503, December 2, 1997.
- Lind, C.; Wilkinson, A. P.; Hu, Z. B.; Short, S.; Jorgensen, J. D. *Chem. Mater.* **1998**, *10*, 2335.
- Closmann, C.; Sleight, A. W.; Haygarth, J. C. *J. Solid State Chem.* **1998**, *139*, 424.
- Pryde, A. K. A.; Hammonds, K. D.; Dove, M. T.; Heine, V.; Gale, J. D.; Warren, M. C. *J. Phys.: Condens. Matter* **1996**, *8*, 10973.
- David, W. I. F.; Evans, J. S. O.; Sleight, A. W. *Europhys. Lett.* **1999**, *46*, 661.
- Graham, J.; Wadsley, A. D.; Weymouth, J. H.; Williams, L. S. *J. Am. Ceram. Soc.* **1959**, *42*, 570.
- Palitsyna, S. S.; Mokhosoev, M. V.; Krivobok, V. I. *Bull. Acad. Sci. USSR Div. Chem. Sci.* **1977**, *611*.
- Xing, X. R.; Xing, Q. F.; Yu, R. B.; Meng, J.; Chen, J.; Liu, G. R. *Physica B* **2006**, *371*, 81.
- Colin, J. A.; Camper, D. V.; Gates, S. D.; Simon, M. D.; Witker, K. L.; Lind, C. *J. Solid State Chem.* **2007**, *180*, 3504.
- Kozy, L. C.; Tahir, M. N.; Lind, C.; Tremel, W. *J. Mater. Chem.* **2009**, *19*, 2760.
- Duan, N.; Kameswari, U.; Sleight, A. W. *J. Am. Chem. Soc.* **1999**, *121*, 10432.
- Lind, C. Negative Thermal Expansion Materials Related to Cubic Zirconium Tungstate. Ph.D. Thesis, Georgia Institute of Technology, Atlanta, GA, 2001.

JA101475F